

**P-05-217**

## **Forsmark site investigation**

### **Borehole KFM08A**

#### **Triaxial compression test of intact rock**

Lars Jacobsson  
SP Swedish National Testing and Research Institute

December 2005

**Svensk Kärnbränslehantering AB**

Swedish Nuclear Fuel  
and Waste Management Co  
Box 5864

SE-102 40 Stockholm Sweden

Tel 08-459 84 00

+46 8 459 84 00

Fax 08-661 57 19

+46 8 661 57 19



## **Forsmark site investigation**

### **Borehole KFM08A**

#### **Triaxial compression test of intact rock**

Lars Jacobsson

SP Swedish National Testing and Research Institute

December 2005

*Keywords:* Rock mechanics, Triaxial compression test, Elasticity parameters, Stress-strain curve, Post-failure behaviour, AP PF 400-05-058.

This report concerns a study which was conducted for SKB. The conclusions and viewpoints presented in the report are those of the author and do not necessarily coincide with those of the client.

A pdf version of this document can be downloaded from [www.skb.se](http://www.skb.se)

## Abstract

Triaxial compression tests with constant confining pressure, containing the complete loading response beyond compressive failure, so called post-failure tests, were carried out on 6 water saturated specimens of intact rock from borehole KFM08A in Forsmark. The cylindrical specimens were taken from drill cores at depth levels ranging between 326–619 m borehole length. The sampled rock type was medium-grained granite. The elastic properties, represented by the Young's modulus and the Poisson ratio, and the compressive strength were deduced from these tests. The wet density of the specimens was determined prior to the mechanical tests. The specimens were photographed before and after the mechanical testing.

The measured density for the water saturated specimens was  $2,660 \text{ kg/m}^3$ . Three confining pressure levels were used, 5, 10 and 20 MPa, and the peak values of the axial compressive stress were in the range 310.7–524.5 MPa. The elastic parameters were determined at a load corresponding to 50% of the failure load and it was found that Young's modulus was in the range 66.2–73.0 GPa with a mean value of 69.6 GPa and the Poisson ratio was in the range of 0.22–0.26 with a mean value of 0.23. It was seen from the mechanical tests that the material in the specimens responded in a brittle way.

## Sammanfattning

Triaxiella kompressionsprov med belastning upp till brott och efter brott, så kallade ”post-failure tests”, har genomförts på 6 stycken vattenmättade cylindriska provobjekt av intakt berg. Provobjekten har tagits från en borrhärlängd mellan 326–619 m borrhålsdjup i Forsmark vid djupnivåer mellan 326–619 m borrhålsdjup. Bergarten var medelkornig granit. De elastiska egenskaperna, representerade av elasticitetsmodulen och Poissons tal, har bestämts ur försöken. Bergmaterialets densitet i vått tillstånd hos proverna mättes upp före de mekaniska proven. Provobjekten fotograferades såväl före som efter de mekaniska proven.

Den uppmätta densiteten hos de vattenmättade proven var  $2\,660\text{ kg/m}^3$ . Tre olika celltryck användes vid triaxialproven, 5, 10 och 20 MPa, och toppvärdena för den axiella kompressiva spänningen låg mellan 310,7–524,5 MPa. De elastiska parametrarna bestämdes vid en last motsvarande 50 % av topplasten vilket gav en elasticitetsmodul mellan 66,2–73,0 GPa med ett medelvärde på 69,6 GPa och Poissons tal mellan 0,22–0,26 med ett medelvärde på 0,23. Vid belastningsförsöken kunde man se att materialet i provobjekten hade ett sprött beteende.

# Contents

<b>1</b>	<b>Introduction</b>	7
<b>2</b>	<b>Objective</b>	9
<b>3</b>	<b>Equipment</b>	11
3.1	Specimen preparation and density measurement	11
3.2	Mechanical testing	11
<b>4</b>	<b>Execution</b>	13
4.1	Description of the specimens	13
4.2	Specimen preparation and density measurement	13
4.3	Mechanical testing	14
4.4	Data handling	15
4.5	Analyses and interpretation	15
4.6	Nonconformities	16
<b>5</b>	<b>Results</b>	17
5.1	Results for each individual specimen	17
5.2	Results for the entire test series	29
	<b>References</b>	33
	<b>Appendix A</b>	35
	<b>Appendix B</b>	37

# 1 Introduction

This document reports performance and results of triaxial compression tests, with loading beyond the failure point into the post-failure regime, on water-saturated specimens sampled from borehole KFM08A at Forsmark, see map in Figure 1-1. The tests were carried out in the material and rock mechanics laboratories at the Department of Building Technology and Mechanics at the Swedish National Testing and Research Institute (SP). The activity is part of the site investigation programme at Forsmark managed by SKB (The Swedish Nuclear Fuel and Waste Management Company).

The controlling documents for the activity are listed in Table 1-1. Both Activity Plan and Method Descriptions are SKB's internal controlling documents, whereas the Quality Plan referred to in the table is an SP internal controlling document.

Borehole KFM08A, see Figure 1-1, is a telescopic drilled borehole inclined c 60° from the horizontal plane and with a total length of 1,001.19 m. The borehole section 0–100.55 m is percussion drilled, whereas section 100.55–1,001.19 m is core drilled.

SKB supplied SP with rock cores which arrived at SP in August 2005 and were tested during November 2005. Cylindrical specimens were cut from the cores and selected based on the preliminary core logging with the strategy to primarily investigate the properties of the dominant rock type. The method description SKB MD 190.003 was followed both for sampling and for the triaxial compression tests, whereas the density determinations were performed in compliance with method description SKB MD 160.002.

As to the specimen preparation, the end surfaces of the specimens were grinded in order to comply with the required shape tolerances. The specimens were kept stored in water, with a minimum of 7 days, up to testing. This yields a water saturation, which is intended to resemble the in-situ moisture condition. The density was determined on each specimen and the triaxial compression tests were carried out at this moisture condition at different confining pressures. The specimens were photographed before and after the mechanical testing.

The triaxial compression tests were carried out using radial strain as the feed-back signal in order to obtain the complete response in the post-failure regime on brittle specimens as described in the method description SKB MD 190.003 and in the ISRM suggested method /1/. The axial  $\varepsilon_a$  and radial strain  $\varepsilon_r$ , together with the axial stress  $\sigma_a$  were recorded during the test. The peak value of the axial compressive stress  $\sigma_c$  was determined at each test. Furthermore, two elasticity parameters, Young's modulus  $E$  and Poisson ratio  $\nu$ , were deduced from the tangent properties at 50% of the peak load. Diagrams with the volumetric and crack volumetric strain versus axial stress are reported. These diagrams can be used to determine crack initiation stress  $\sigma_i$  and the crack damage stress  $\sigma_d$ , cf /2, 3/.

**Table 1-1. Controlling documents for performance of the activity.**

<b>Activity Plan</b>	<b>Number</b>	<b>Version</b>
KFM08A. Bergmekaniska och termiska laboratoriebestämningar	AP PF 400-05-058	1.0
<b>Method Descriptions</b>	<b>Number</b>	<b>Version</b>
Triaxial compression test for intact rock	SKB MD 190.003	2.0
Determining density and porosity of intact rock	SKB MD 160.002	2.0
<b>Quality Plan</b>		
SP-QD 13.1		

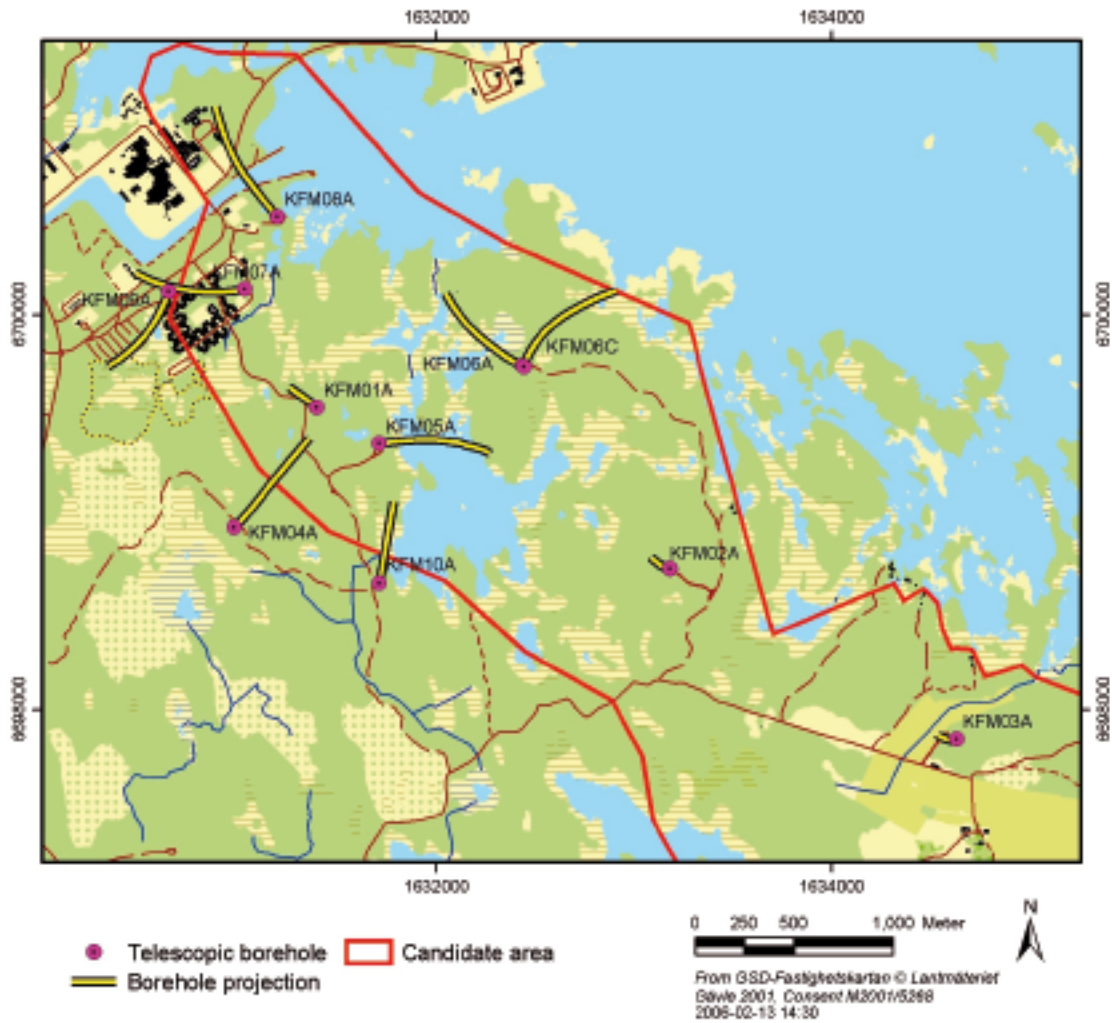


*Figure 1-1. Location of deep core drilled boreholes completed up to December 2005 within or close to the Forsmark candidate area. The projection of each borehole on the horizontal plane at top of casing is also shown in the figure.*

## **2 Objective**

The purpose of the testing was to determine the compressive strength and the elastic properties, represented by Young's modulus and the Poisson ratio, of confined cylindrical intact rock cores at different confining pressures. Moreover, the specimens had a water content corresponding to the in-situ conditions. The loading was carried out into the post-failure regime in order to study the mechanical behaviour of the rock after cracking, enabling determination of the brittleness and residual strength.

The results from the tests are going to be used in the site descriptive rock mechanics model, which will be established for the candidate area selected for site investigations at Forsmark.



## 3 Equipment

### 3.1 Specimen preparation and density measurement

A circular saw with a diamond blade was used to cut the specimens to their final lengths. The surfaces were then grinded after cutting in a grinding machine in order to achieve a high-quality surface for the axial loading that complies with the required tolerances. The measurements of the specimen dimensions were made with a sliding calliper. Furthermore, the tolerances were checked by means of a dial indicator and a stone face plate. The specimen preparation is carried out in accordance with ASTM 4543-01 /4/.

The specimens and the water were weighed using a scale for weight measurements. A thermometer was used for the water temperature measurements. The calculated wet density was determined with an uncertainty of  $\pm 4 \text{ kg/m}^3$ .

### 3.2 Mechanical testing

The mechanical tests were carried out in a servo controlled testing machine specially designed for rock tests, see Figure 3-1. The system consists of a load frame, a hydraulic pump unit, a controller unit and various sensors. The communication with the controller unit is accomplished by special testing software run on a PC connected to the controller. The load frame is characterized by a high stiffness and is supplied with a fast responding actuator, cf the ISRM suggested method /1/. Furthermore, the sensors, the controller and the servo valves are rapidly responding components. The machine is equipped with a pressure vessel in which the specimens are tested under a confinement pressure. A thin rubber membrane is mounted on the specimen in order to seal the specimen from the oil that is used as the confinement medium, cf Figure 3-2. The axial load is determined using a load cell, which is located inside the pressure vessel and has a maximum capacity of 1.5 MN. The uncertainty of the load measurement is less than 1%.

The axial and circumferential (radial) deformation of the rock specimen was measured. The rock deformation measurement systems are based on miniature LVDTs, which have a measurement range of  $\pm 2.5 \text{ mm}$ . The LVDTs were calibrated by means of a micrometer and they displayed an accuracy of  $\pm 2.5\%$  within a  $\pm 2 \text{ mm}$  range. The axial deformation measurement system comprises two aluminium rings attached on the specimen, placed approximately at  $\frac{1}{4}$  and  $\frac{3}{4}$  of the specimen height, cf Figures 3-2 and 4-1. Two LVDTs mounted on the rings are used to measure the distance change between the rings on opposite sides of the specimen. The rings are supplied with three adjustable spring-loaded screws, each with a rounded tip, pointing towards the specimen with 120 degrees division. The rings are mounted directly on the rubber membrane. The pre-load of the screws fixates the rings. The position of the frame piston was also stored during the test in order to permit a possibility for comparison with the measurements made with the measurement system that was based on the displacement of the rings.

The radial deformation was obtained by using a chain mounted around the specimen at mid-height, see Figure 3-2. The change of the chain-opening gap was measured by means of one LVDT and the circumferential and thereby also the radial deformation could be obtained. See Appendix A.

The specimens were photographed with a 4.0 Mega pixel digital camera at highest resolution and the photographs were stored in a jpeg-format.



**Figure 3-1.** Left: Digital controller unit, pressure cabinet with cell pressure intensifier and oil reservoir inside, and the load frame with closed cell (pressure vessel). Right: Bottom of the cell is lowered. The specimen is instrumented and ready for inserting in the cell.



**Figure 3-2.** Left: Rings and LVDTs for axial deformation measurement. Right: Specimen and loading platens sealed with a rubber membrane. Devices for axial and circumferential deformation measurements are attached.

## 4 Execution

The water saturation and determination of the density of the wet specimens were made in accordance with the method description SKB MD 160.002 (SKB internal controlling document). This includes determination of density in accordance to ISRM /5/ and water saturation by SS-EN 13755 /6/. The triaxial compression tests were carried out in compliance with the method description SKB MD 190.003 (SKB internal controlling document). The test method is based on the ISRM suggested methods /1/ and /7/.

### 4.1 Description of the specimens

The rock type characterisation was made according to Strähle /8/ using the SKB mapping system (Boremap). The identification marks, upper and lower sampling depth (Secup and Seclow) and the rock type are shown in Table 4-1.

### 4.2 Specimen preparation and density measurement

The specimens were cut to a prescribed length and the end surfaces of the specimens were grinded in order to comply with the required shape tolerances. Further, the specimens were put in water and kept stored in water for 8 days, up to density determination. The temperature of the water was 21.0°C, which equals to a water density of 998.0 kg/m<sup>3</sup>, when the determination of the wet density of the rock specimens was carried out.

An overview of the activities during the specimen preparation is shown in the step-by step description in Table 4-2.

**Table 4-1. Specimen identification, sampling level (borehole length), confining pressure at the triaxial tests and rock type for all specimens.**

Identification	Secup [m]	Seclow [m]	Confining pressure [MPa]	Rock type
KFM08A-115-1	326.25	326.41	5	Medium-grained granite
KFM08A-115-4	398.48	398.63	10	Medium-grained granite
KFM08A-115-6	523.64	523.78	20	Medium-grained granite
KFM08A-115-8	523.96	524.11	5	Medium-grained granite
KFM08A-115-9	618.11	618.26	10	Medium-grained granite
KFM08A-115-10	618.26	618.42	20	Medium-grained granite

**Table 4-2. Activity sequence during the specimen preparation.**

Step	Activity
1	The drill cores were marked where the specimens are to be taken.
2	The specimens were cut to the specified length according to markings and the cutting surfaces were grinded.
3	The tolerances were checked: parallel and perpendicular end surfaces, smooth and straight circumferential surface.
4	The diameter and height were measured three times each. The respective mean value determines the dimensions that are reported.
5	The specimens were then water saturated according to the method described in SKB MD 160.002 and were stored for minimum 7 days in water, whereupon the wet density was determined.

### 4.3 Mechanical testing

The specimens had been stored during 8–10 days in water when the triaxial compression tests were carried out. The functionality of the triaxial testing system was checked, by performing tests on other cores with a similar rock type before the tests described in this report started. A check-list was filled in successively during the work in order to confirm that the different specified steps had been carried out. Moreover, comments were made upon observations made during the mechanical testing that are relevant for the interpretation of the results. The check-list form is an SP internal quality document.

An overview of the activities during the mechanical testing is shown in the step-by step description in Table 4-3.

**Table 4-3. Activity sequence during the mechanical testing.**

Step	Activity
1	Digital photos were taken on each specimen prior to the mechanical testing.
2	The specimen was put in testing position and centred between the loading platens.
3	A rubber membrane was mounted on the specimen and the devices for measuring axial and circumferential deformations were attached to the specimen on top of the rubber membrane.
4	The core on each LVDT was adjusted by means of a set screw to the correct initial position. This was done so that the optimal range of the LVDTs can be used for the deformation measurement.
5	The triaxial cell was closed and filled with oil whereby a cell pressure of 0.6 MPa is applied.
6	The frame piston was brought down into contact with the specimen with a force corresponding to a deviatoric stress of 0.6 MPa. The cell pressure was then raised to the specified level and at the same time keeping the deviatoric stress constant.
7	The deformation measurement channels were zeroed in the test software.
8	The loading was started and the initial loading rate was set to a radial strain rate of $-0.025\%/min$ . The loading rate was increased after reaching the post-failure region. This was done in order to prevent the total time for the test to become too long.
9	The test was stopped either manually, when the test had proceeded long enough to reveal the post-failure behaviour, or after severe cracking had occurred and it was judged that very little residual axial loading capacity was left in the specimen.
10	The oil pressure was brought down to zero and the oil was poured out of the cell. The cell was opened and the specimen removed.
11	Digital photos were taken on each specimen after the mechanical testing.

## 4.4 Data handling

The test results were exported as text files from the test software and stored in a file server on the SP computer network after each completed test. The main data processing, in which the elastic moduli were computed and the peak stress was determined, has been carried out in the program MATLAB /9/. Moreover, MATLAB was used to produce the diagrams shown in Section 5.1 and in Appendix B. The summary of results in Section 5.2 with tables containing mean value and standard deviation of the different parameters and diagrams was provided using MS Excel. MS Excel was also used for reporting data to the SICADA database.

## 4.5 Analyses and interpretation

As to the definition of the different results parameters we begin with the axial stress  $\sigma_a$ , which is defined as

$$\sigma_a = \frac{F}{A}$$

where  $F$  is the axial force acting on the specimen, and  $A$  is the specimen cross section area. The pressure vessel (triaxial cell) filled with oil is pressurized with a cell (confining) pressure  $p$ . This implies that the specimen, located inside the pressure vessel, becomes confined and attains a radial stress  $\sigma_r$  equal to the confining pressure  $p$ . The (effective) deviatoric stress is defined as

$$\sigma_{dev} = \sigma_a - \sigma_r$$

The peak value of the axial stress during a test is representing the triaxial compressive strength  $\sigma_c$ , for the actual confining pressure used in the test, see the results presentation.

The average value of the two axial displacement measurements on opposite sides of the specimen is used for the axial strain calculation. The recorded deformation  $\delta_{local}$  represents a local axial displacement between the points approximately at  $\frac{1}{4}$  and  $\frac{3}{4}$  of the specimen height, cf Figure 4-1. The axial strain is defined as

$$\varepsilon_a = \delta_{local} / L_{local}$$

where  $L_{local}$  is the distance between the rings before loading.

The radial deformation is measured by means of a chain mounted around the specimen at mid-height, see Figure 3-2. The change of chain opening gap is measured by means of one LVDT. This measurement is used to compute the radial strain  $\varepsilon_r$ , see Appendix A. Moreover, the volumetric strain  $\varepsilon_{vol}$  is defined as

$$\varepsilon_{vol} = \varepsilon_a + 2\varepsilon_r$$

The stresses and the strains are defined as positive in compressive loading and deformation. The elasticity parameters are defined by the tangent Young's modulus  $E$  and tangent Poisson ratio  $\nu$  as

$$E = \frac{\sigma_a(0.60\sigma_c) - \sigma_a(0.40\sigma_c)}{\varepsilon_a(0.60\sigma_c) - \varepsilon_a(0.40\sigma_c)}$$
$$\nu = -\frac{\varepsilon_r(0.60\sigma_c) - \varepsilon_r(0.40\sigma_c)}{\varepsilon_a(0.60\sigma_c) - \varepsilon_a(0.40\sigma_c)}$$

The tangents were evaluated with values corresponding to an axial load between 40% and 60% of the axial peak stress  $\sigma_c$ .

A closure of present micro cracks will take place initially during confinement and axial loading. Development of new micro cracks will start when the axial load is further increased and

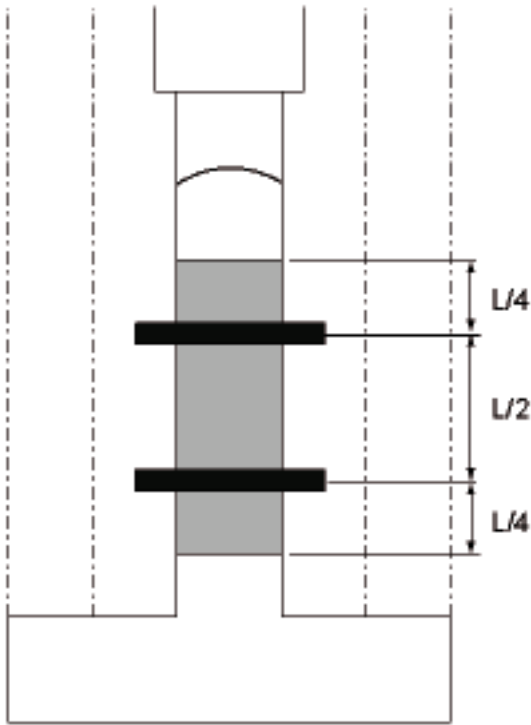


**Figure 4-1.** Sketch showing the triaxial cell with the rock specimen (grey) with height  $L$  and the position of the rings (black) used for the axial deformation measurements. The membrane is omitted in the figure for simplicity.

axial stress reaches the crack initiation stress  $\sigma_i$ . The crack growth at this stage is as stable as increased loading is required for further cracking. A transition from a development of micro cracks to macro cracks will take place when the axial load is further increased. At a certain stress level the crack growth becomes unstable. The stress level when this happens is denoted the crack damage stress  $\sigma_d$ , cf /2, 3/. In order to determine the stress levels we look at the volumetric strain.

By subtracting the elastic volumetric strain  $\varepsilon_{vol}^e$  from the total volumetric strain, a volumetric strain corresponding to the crack volume is obtained  $\varepsilon_{vol}^{cr}$ . This has been denoted calculated crack volumetric strain in the literature, cf /2, 3/. We thus have

$$\varepsilon_{vol}^{cr} = \varepsilon_{vol} - \varepsilon_{vol}^e$$

Assuming linear elasticity leads to

$$\varepsilon_{vol}^{cr} = \varepsilon_{vol} - \frac{1-2\nu}{E}(\sigma_a - \sigma_r)$$

Experimental investigations have shown that the crack initiation stress  $\sigma_i$  coincides with the onset of increase of the calculated crack volume, cf /2, 3/. The same investigations also indicate that the crack damage stress  $\sigma_d$  can be defined as the axial stress at which the total volume starts to increase, i.e. when a dilatant behaviour is observed.

## 4.6 Nonconformities

The testing was conducted according to the method description except for one deviation. The circumferential strains were determined within a relative error of 1.5%, which is larger than what is specified in the ISRM-standard /1/.

The activity plan was followed with no departures.

## 5 Results

The results of the individual specimens are presented in Section 5.1 and a summary of the results is given in Section 5.2. The reported parameters are based on unprocessed raw data obtained from the testing and were reported to the SICADA database, where they are traceable by the activity plan number. These data together with the digital photographs of the individual specimens were stored on a CD and handed over to SKB. The handling of the results follows SDP-508 (SKB internal controlling document) in general.

### 5.1 Results for each individual specimen

The cracking is shown in pictures taken on the specimens with comments on observations made during testing. The elasticity parameters have been evaluated by using the results from the local deformation measurements. Red rings are superposed on the graphs indicating every five minutes of the progress of testing. The results for the individual specimens are as follows:

**Specimen ID:** KFM08A-115-1

Before mechanical test



<b>Diameter</b> [mm]	<b>Height</b> [mm]	<b>Density</b> [kg/m <sup>3</sup> ]
51.0	126.3	2,660
<b>Comments</b>	A v-shaped shear failure is observed.	

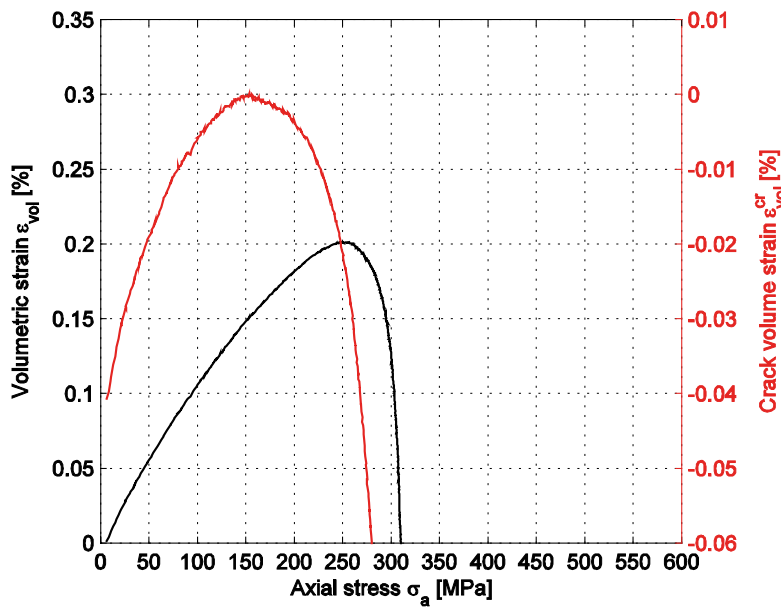
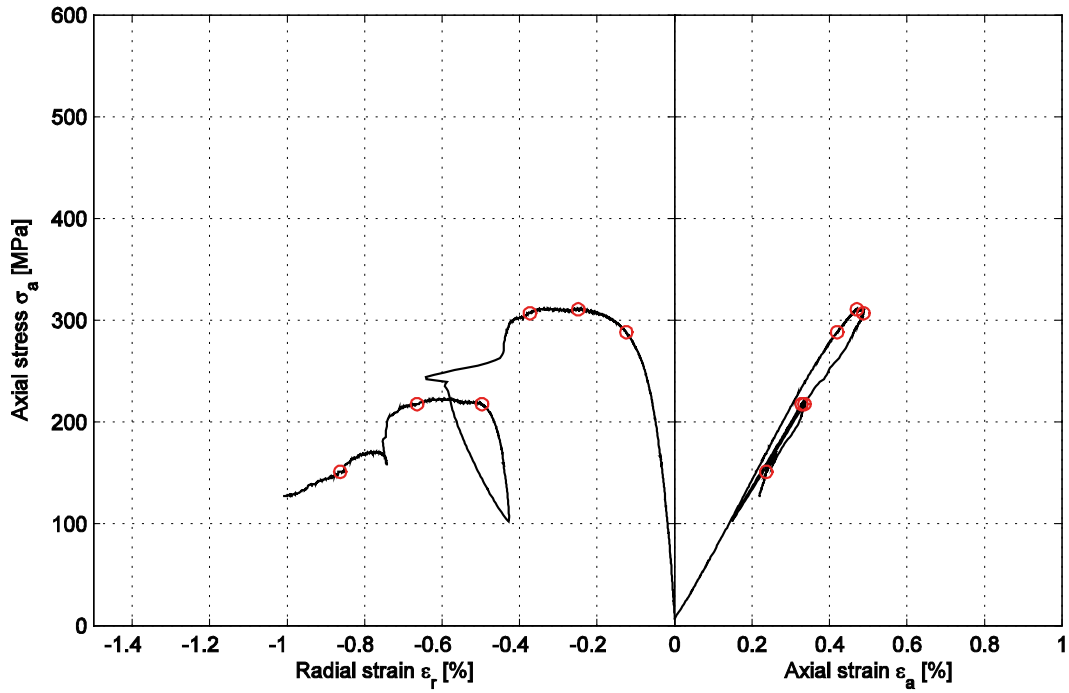
Specimen ID: KFM08A-115-01

Youngs Modulus (E): 73 [GPa]

Cell pressure: 5 [MPa]

Poisson Ratio ( $\nu$ ): 0.23 [-]

Axial peak stress ( $\sigma_p$ ): 311.2 [MPa]





**Specimen ID:** KFM08A-115-4

Before mechanical test

After mechanical test



<b>Diameter</b> [mm]	<b>Height</b> [mm]	<b>Density</b> [kg/m <sup>3</sup> ]
50.9	126.4	2,660

**Comments** One major v-shaped failure is observed. One of the shear bands follows the foliation. In addition, smaller shear cracks oriented along the foliation are also observed.

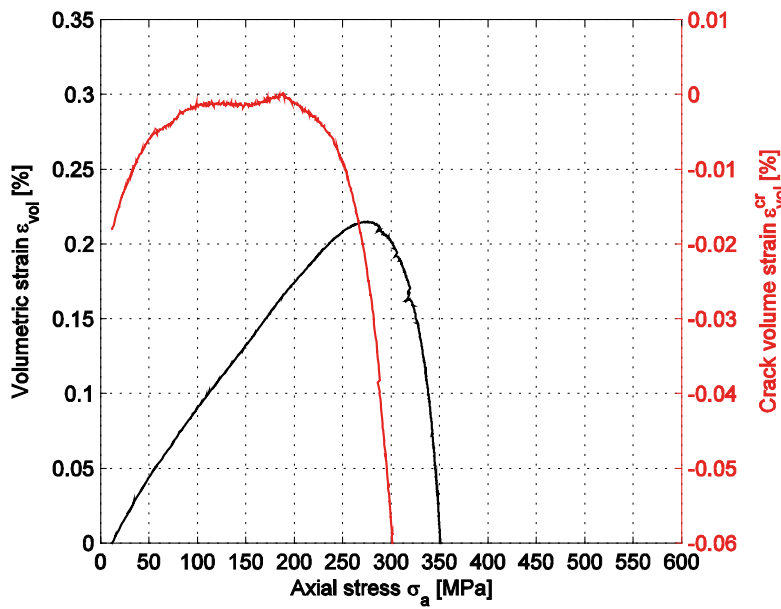
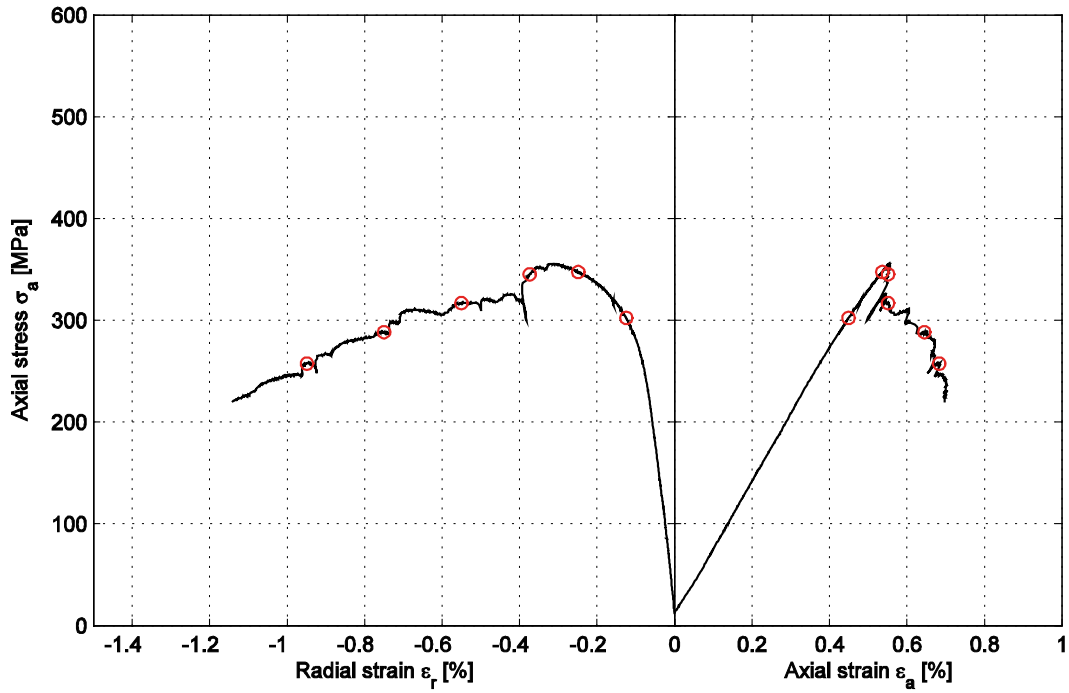
Specimen ID: KFM08A-115-04

Youngs Modulus (E): 66.2 [GPa]

Cell pressure: 10 [MPa]

Poisson Ratio ( $\nu$ ): 0.223 [-]

Axial peak stress ( $\sigma_p$ ): 355.3 [MPa]



**Specimen ID:** KFM08A-115-6

Before mechanical test



After mechanical test



<b>Diameter</b> [mm]	<b>Height</b> [mm]	<b>Density</b> [kg/m <sup>3</sup> ]
50.8	126.4	2,660

**Comments** The specimen failed suddenly and severely resulting in multiple cracks. The membrane was punctured resulting in a leakage.

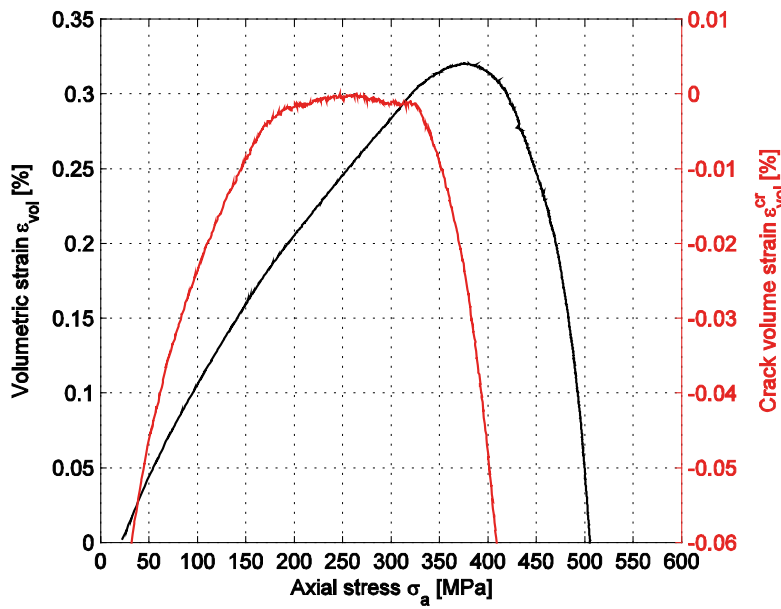
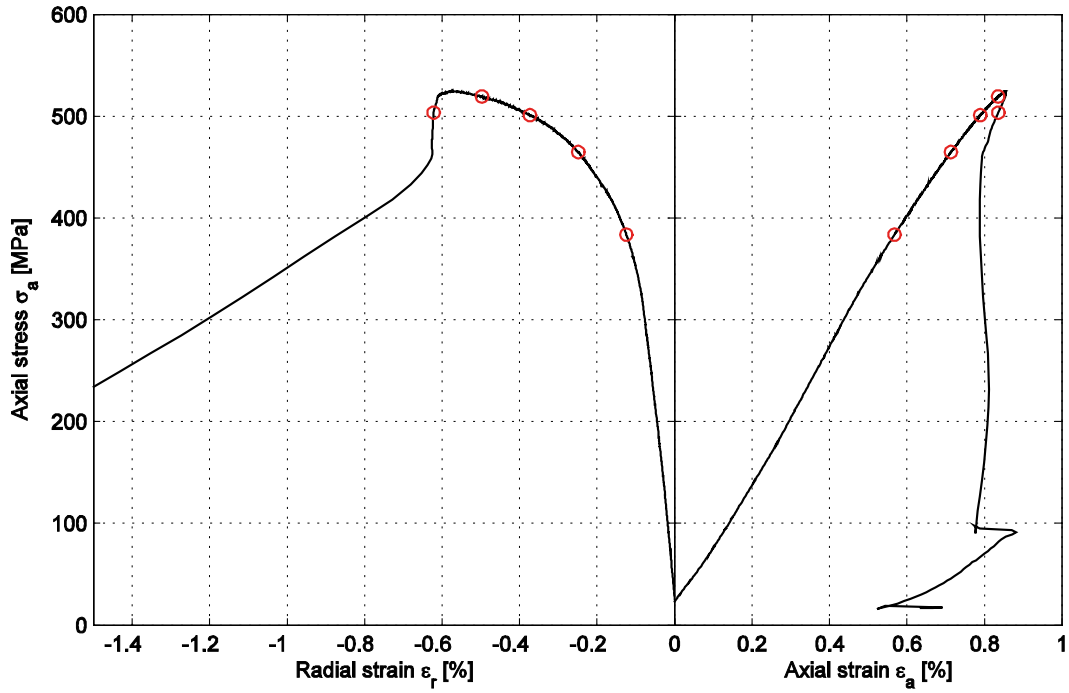
### Specimen ID: KFM08A-115-06

Youngs Modulus (E): 70.8 [GPa]

Cell pressure: 20 [MPa]

Poisson Ratio ( $\nu$ ): 0.225 [-]

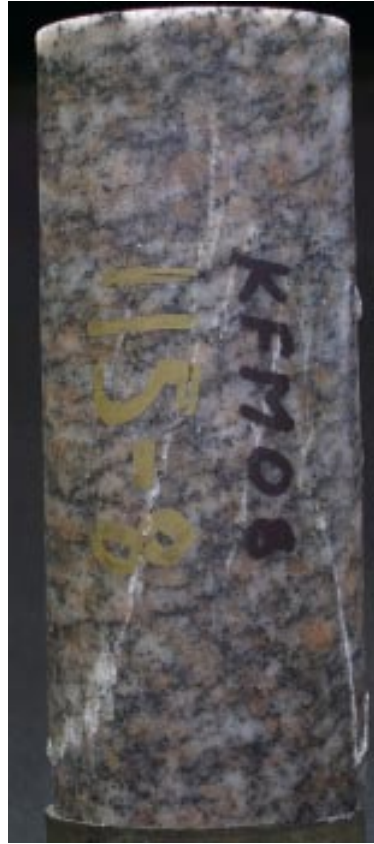
Axial peak stress ( $\sigma_p$ ): 524.5 [MPa]



**Specimen ID:** KFM08A-115-8

Before mechanical test

After mechanical test



**Diameter**  
[mm]  
50.8

**Height**  
[mm]  
125.9

**Density**  
[kg/m<sup>3</sup>]  
2,660

**Comments**

A v-shaped shear failure is observed.

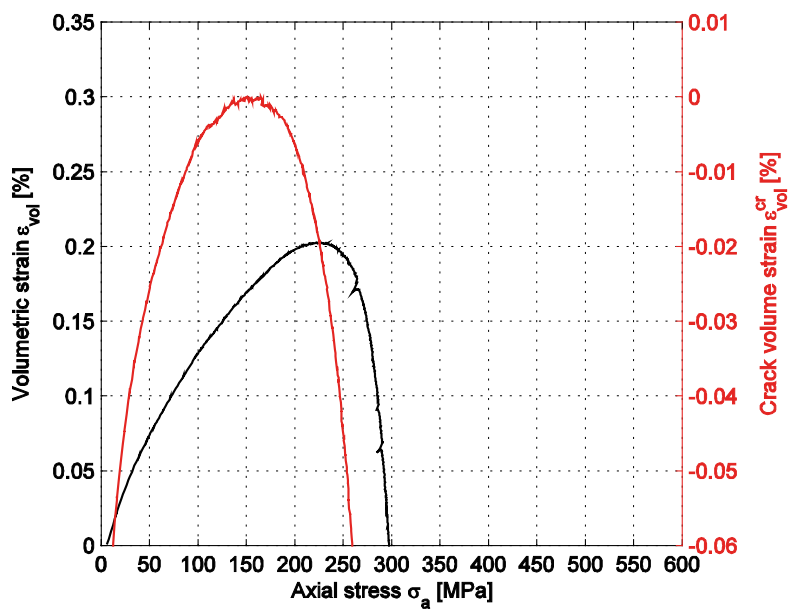
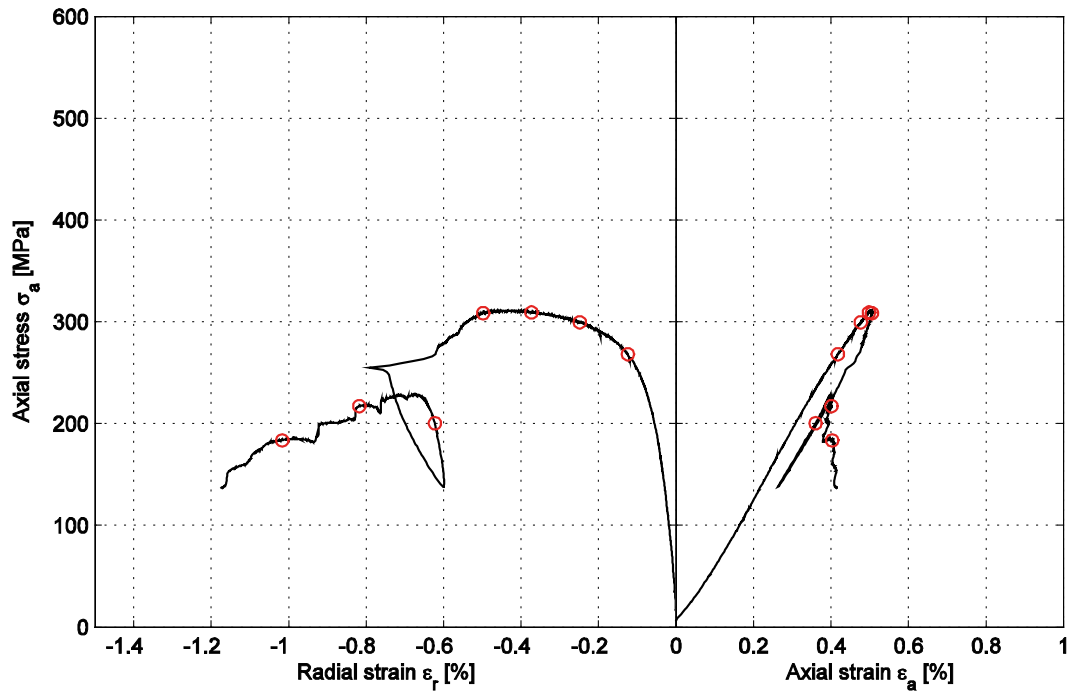
### Specimen ID: KFM08A-115-08

Youngs Modulus (E): 70.2 [GPa]

Cell pressure: 5 [MPa]

Poisson Ratio ( $\nu$ ): 0.255 [-]

Axial peak stress ( $\sigma_c$ ): 310.7 [MPa]





**Specimen ID:** KFM08A-115-9

Before mechanical test

After mechanical test



<b>Diameter</b> [mm]	<b>Height</b> [mm]	<b>Density</b> [kg/m <sup>3</sup> ]
50.8	125.8	2,660

**Comments** The specimen failed suddenly and severely resulting in a v-shaped failure. The membrane was punctured resulting in a leakage.

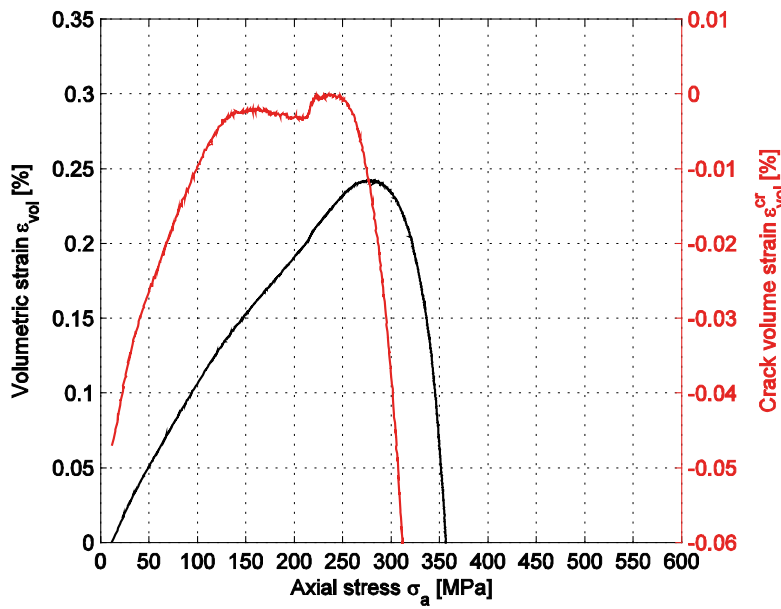
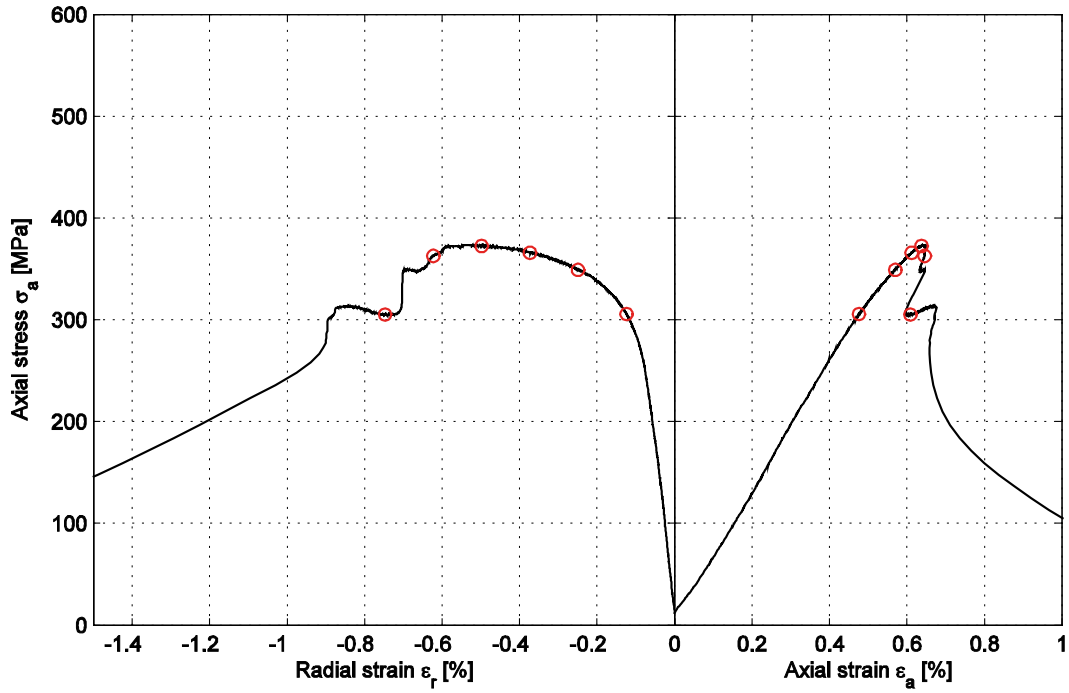
Specimen ID: KFM08A-115-09

Youngs Modulus (E): 66.9 [GPa]

Cell pressure: 10 [MPa]

Poisson Ratio ( $\nu$ ): 0.24 [-]

Axial peak stress ( $\sigma_p$ ): 373.5 [MPa]





**Specimen ID:** KFM08A-115-10

Before mechanical test

After mechanical test



<b>Diameter</b> [mm]	<b>Height</b> [mm]	<b>Density</b> [kg/m <sup>3</sup> ]
50.8	126.4	2,660

**Comments**      A non-symmetric v-shaped failure is observed.

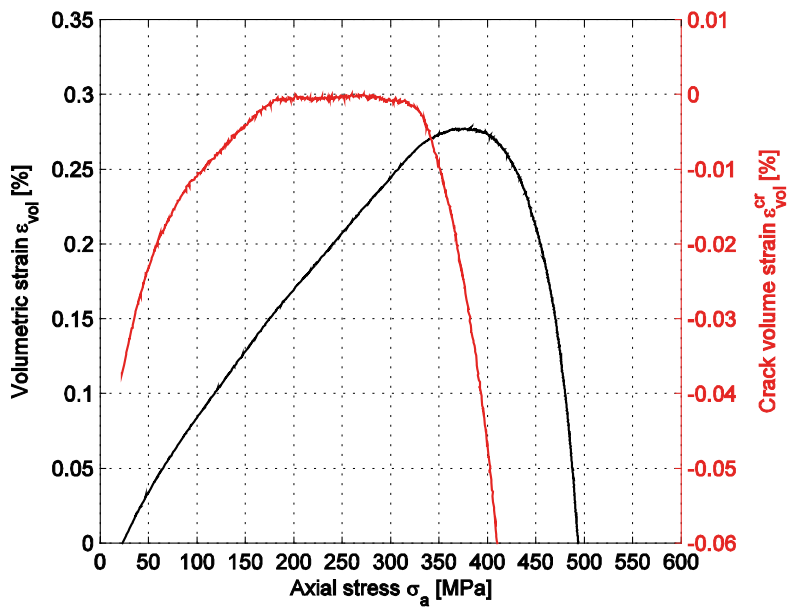
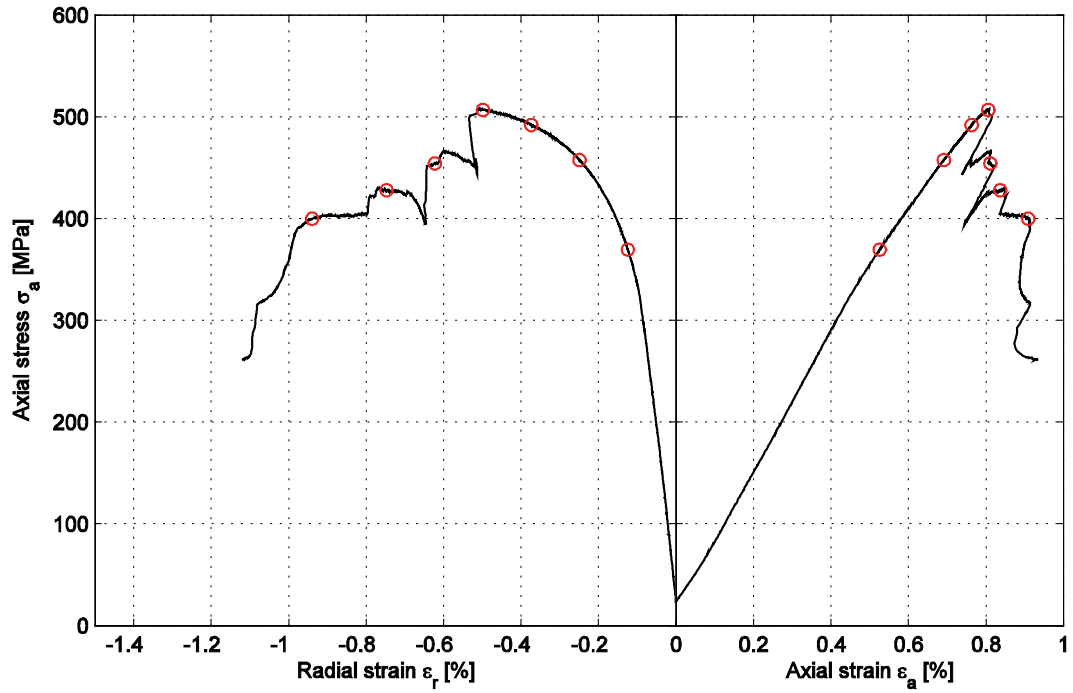
Specimen ID: KFM08A-115-10

Youngs Modulus (E): 70.4 [GPa]

Cell pressure: 20 [MPa]

Poisson Ratio ( $\nu$ ): 0.235 [-]

Axial peak stress ( $\sigma_p$ ): 507.5 [MPa]



## 5.2 Results for the entire test series

A summary of the test results is shown in Tables 5-1 and 5-2. The densities, triaxial compressive strength, the tangent Young's modulus and the tangent Poisson ratio versus sampling level (borehole length), are presented in Figures 5-1 to 5-4.

**Table 5-1. Summary of results.**

Identification	Conf press [MPa]	Density [kg/m <sup>3</sup> ]	Compressive Strength [MPa]	Young's modulus [GPa]	Poisson ratio [-]	Comments
KFM08A-115-1	5	2,660	311.2	73.0	0.23	
KFM08A-115-4	10	2,660	355.3	66.2	0.22	
KFM08A-115-6	20	2,660	524.5	70.8	0.22	
KFM08A-115-8	5	2,660	310.7	70.2	0.26	
KFM08A-115-9	10	2,660	373.5	66.9	0.24	
KFM08A-115-10	20	2,660	507.5	70.4	0.24	

**Table 5-2. Calculated mean values and standard deviation.**

	Density [kg/m <sup>3</sup> ]	Young's modulus [GPa]	Poisson ratio [-]
Mean value	2,660	69.6	0.23
Standard deviation	0.0	2.6	0.01

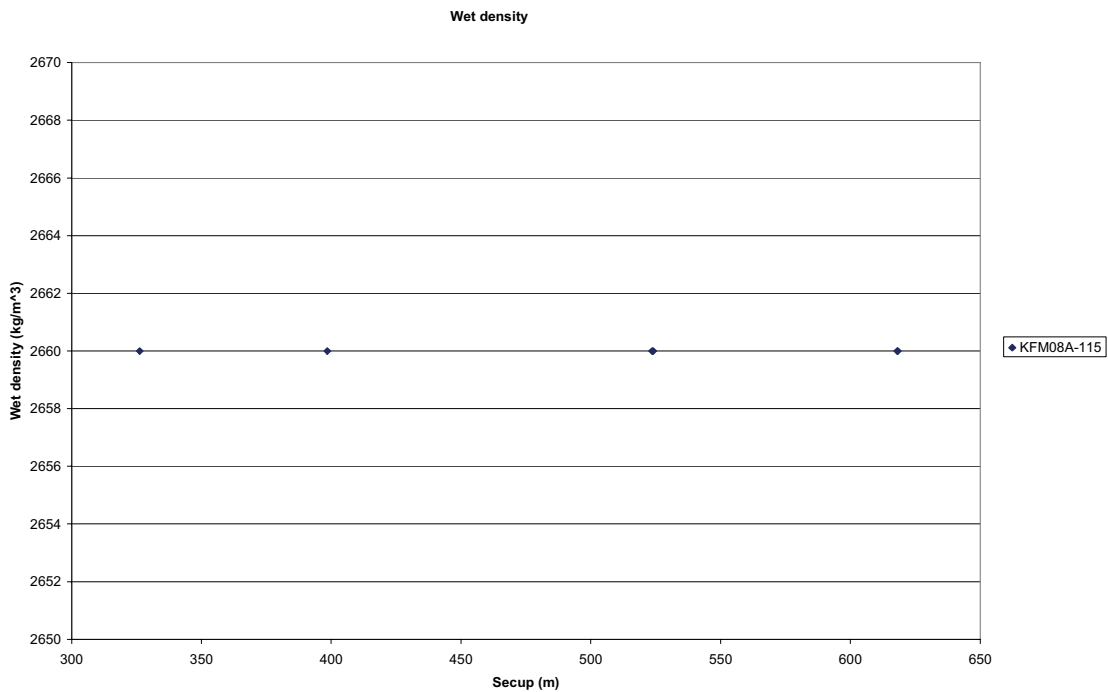


**Figure 5-1. Density versus sampling level (borehole length).**

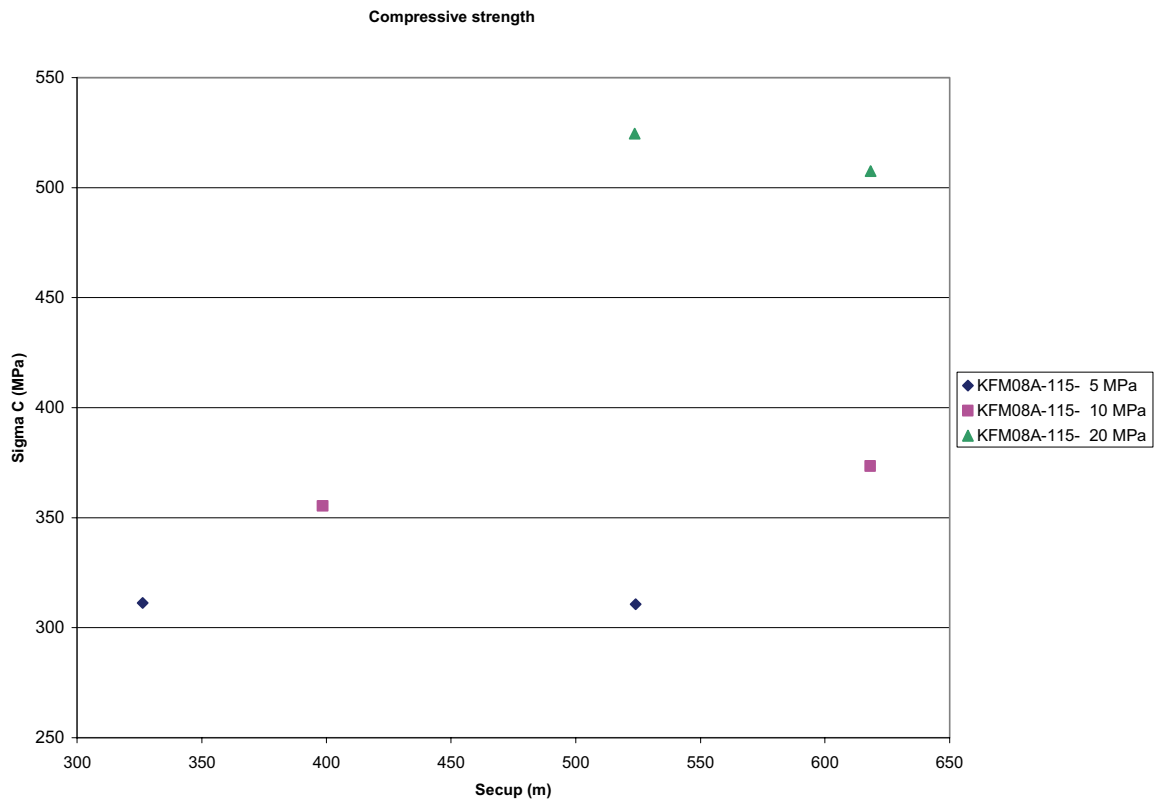


*Figure 5-2. Compressive strength versus sampling level (borehole length).*

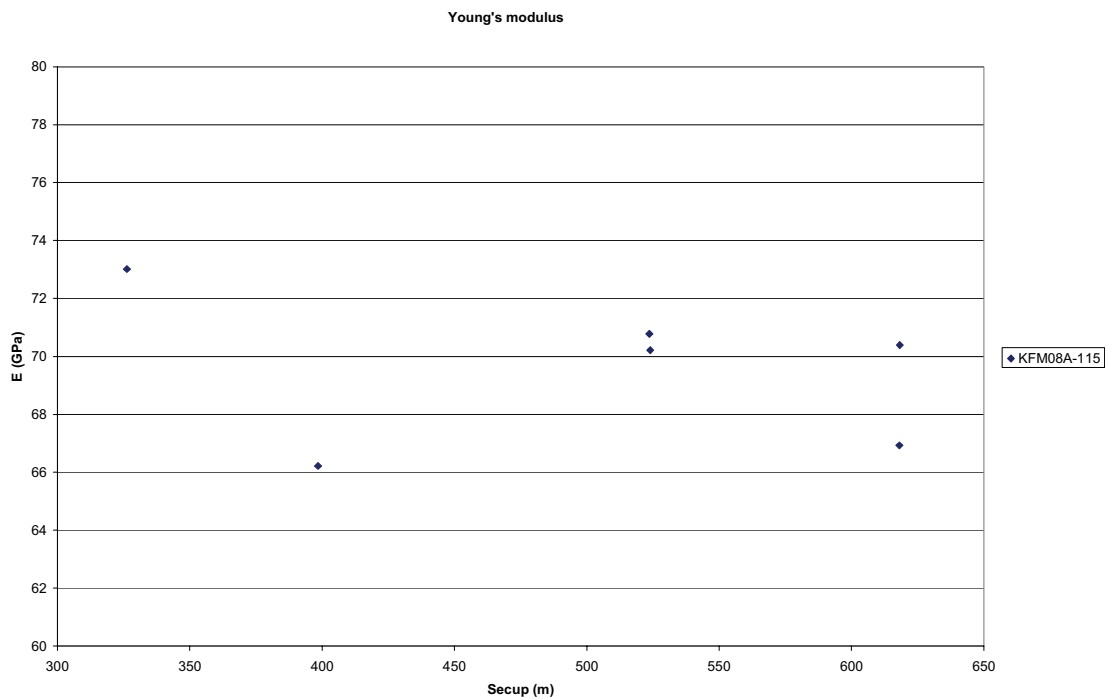


*Figure 5-3. Tangent Young's modulus versus sampling level (borehole length).*

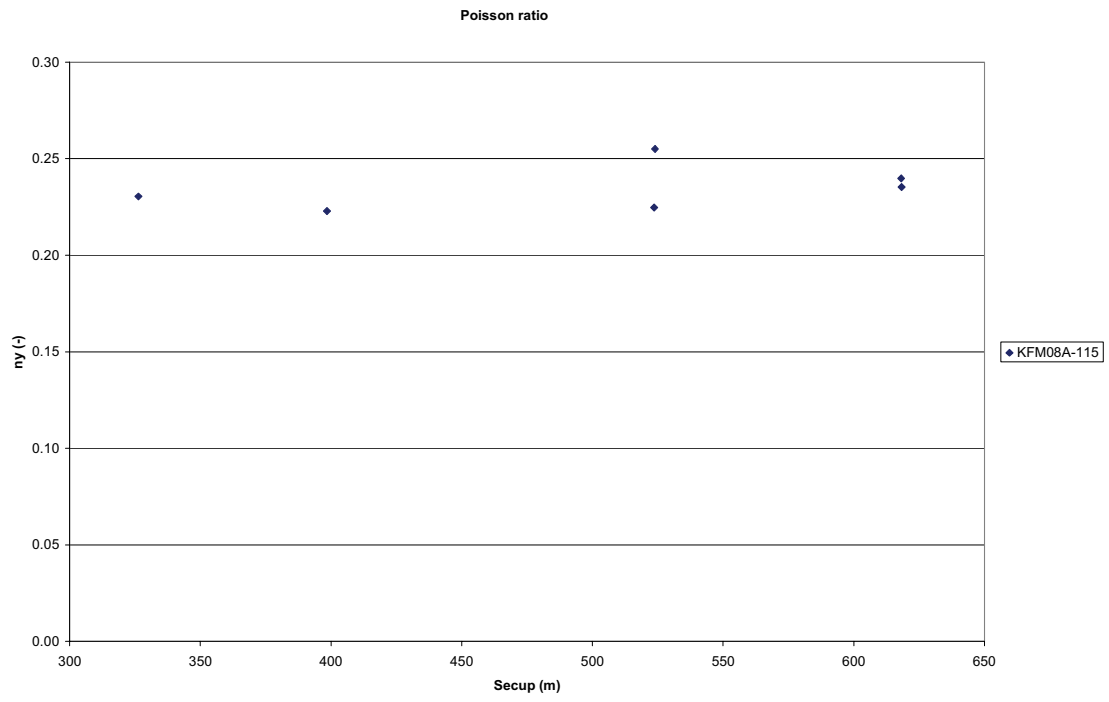


**Figure 5-4.** Tangent Poisson ratio versus sampling level (borehole length).

## References

- /1/ **ISRM, 1999.** Draft ISRM suggested method for the complete stress-strain curve for intact rock in uniaxial compression, *Int. J. Rock. Mech. Min. Sci.* 36(3), pp. 279–289, 1999.
- /2/ **Martin C D, Chandler N A, 1994.** The progressive fracture of Luc du Bonnet granite, *Int. J. Rock. Mech. Min. Sci. & Geomech. Abstr.* 31(6), pp. 643–659, 1994.
- /3/ **Eberhardt E, Stead D, Stimpson B, Read R S, 1998.** Identifying crack initiation and propagation thresholds in brittle rock. *Can. Geotech. J.* 35, pp. 222–233, 1998.
- /4/ **ASTM 4543-01, 2001.** Standard practice for preparing rock core specimens and determining dimensional and shape tolerance, 2001.
- /5/ **ISRM, 1979.** Suggested Method for Determining Water Content. Porosity, Density, Absorption and Related Properties and Swelling and Slake-durability Index Properties, *Int. J. Rock. Mech. Min. Sci. & Geomech. Abstr.* 16(2), pp. 141–156, 1979.
- /6/ **SS-EN 13755.** Natural stone test methods – Determination of water absorption at atmospheric pressure.
- /7/ **ISRM, 1983.** Suggested method for determining the strength of rock material in triaxial compression: Revised version, *Int. J. Rock. Mech. Min. Sci. & Geomech. Abstr.* 20(6), pp. 283–290, 1983.
- /8/ **Stråhle A, 2001.** Definition och beskrivning av parametrar för geologisk, geofysisk och bergmekanisk kartering av berg. In Swedish, SKB R-01-19, Svensk Kärnbränslehantering AB.
- /9/ **MATLAB, 2002.** The Language of Technical computing. Version 6.5. MathWorks Inc., 2002.

## Appendix A

The following equations describe the correct calculation of radial strains when using a circumferential deformation device, see Figure A-1.

$$\varepsilon_r = \frac{\Delta C}{C_i}$$

where

$$C_i = 2 \pi R_i = \text{initial specimen circumference}$$

$$\Delta C = \text{change in specimen circumference} = \frac{\pi \cdot \Delta X}{\sin\left(\frac{\theta_i}{2}\right) + \left(\pi - \frac{\theta_i}{2}\right) \cos\left(\frac{\theta_i}{2}\right)}$$

and

$$\Delta X = \text{change in LVDT reading} = X_i - X_f$$

( $X_i$  = initial chain gap;  $X_f$  = current chain gap)

$$\theta_i = \text{initial chord angle} = 2\pi \frac{L_c}{R_i + r}$$

$L_c$  = chain length (measured from center of one end roller to center of the other end roller)

$r$  = roller radius

$R_i$  = initial specimen radius

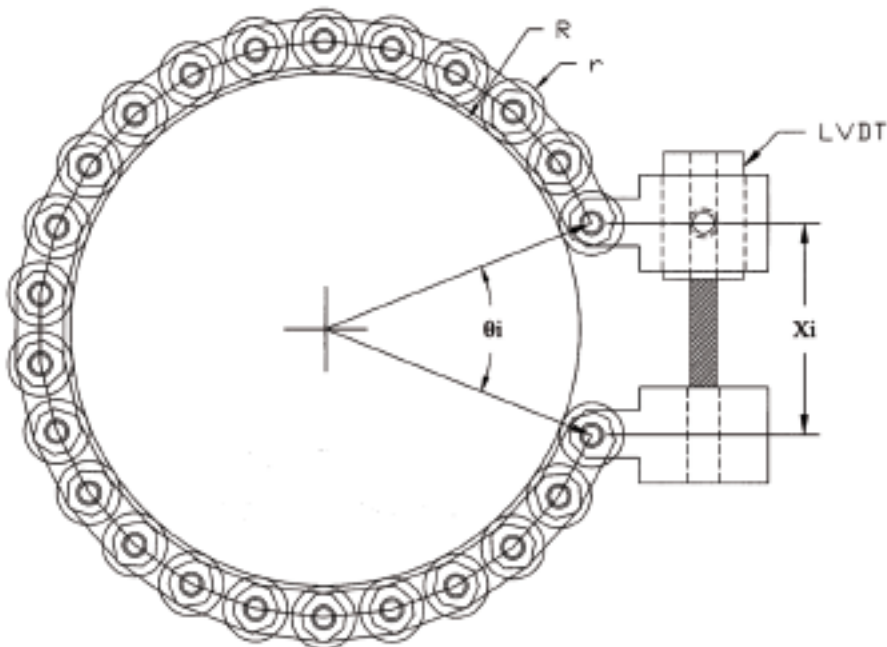
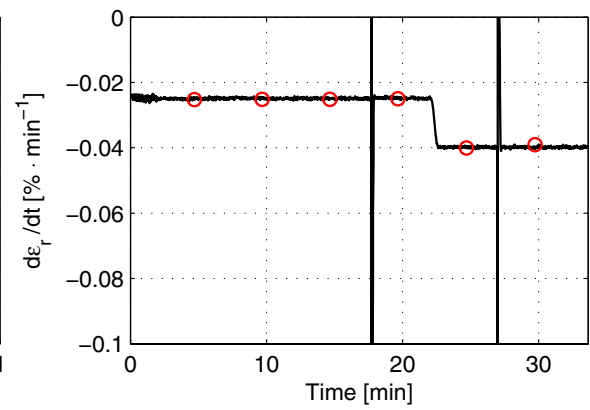
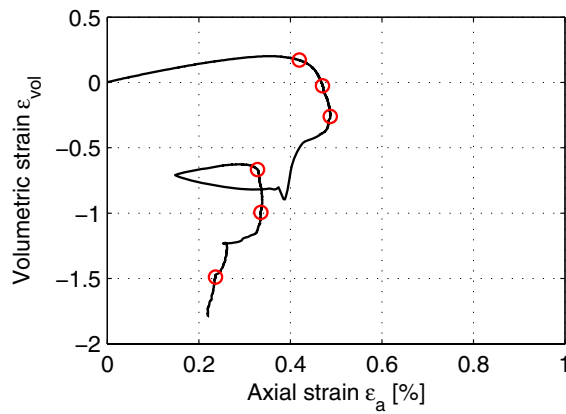


**Figure A-1.** Chain for radial deformation measurement.

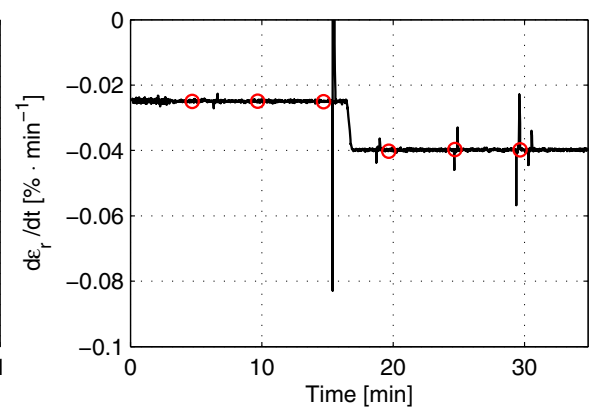
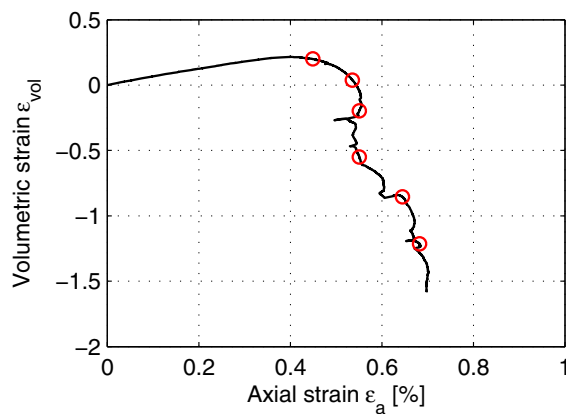
## Appendix B

This Appendix contains complementary results showing the volumetric strain  $\epsilon_{vol}$  versus the axial strain  $\epsilon_a$  and the actual radial strain rate  $d\epsilon_r/dt$  versus time. The complementary results for all tests are shown below.

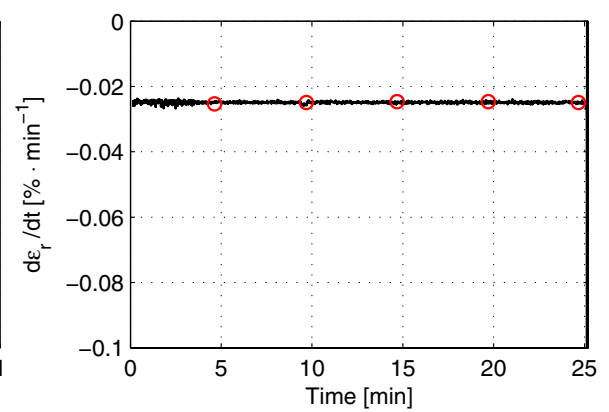
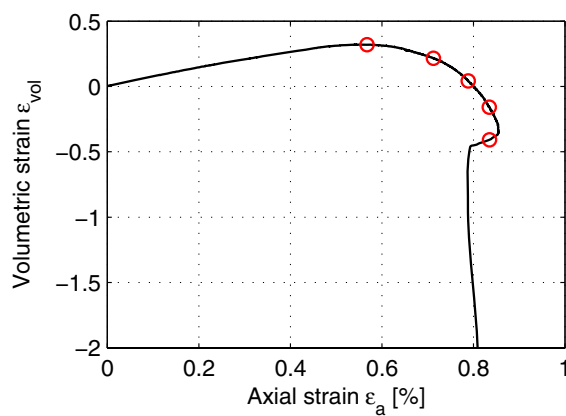
Specimen ID: KFM08A-115-01



Specimen ID: KFM08A-115-04

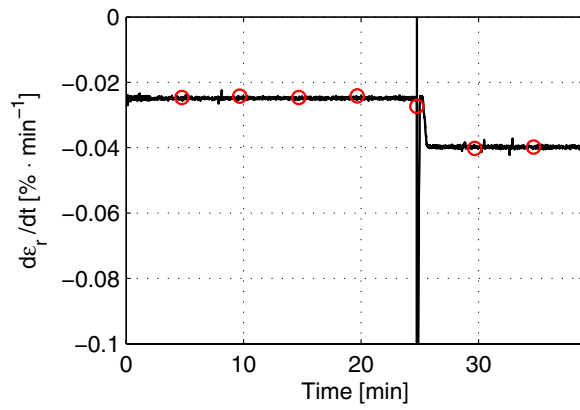
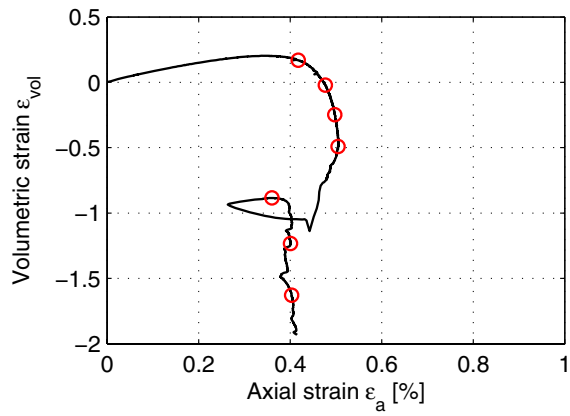


Specimen ID: KFM08A-115-06

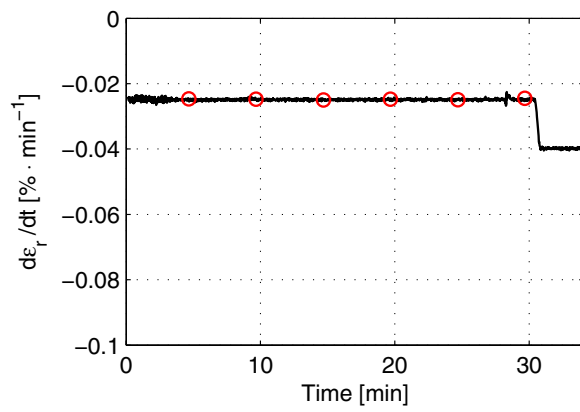
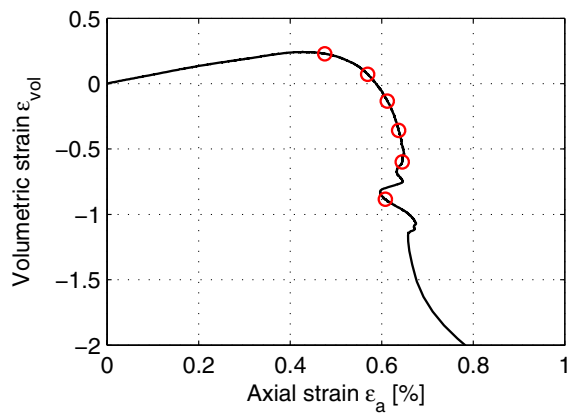




Specimen ID: KFM08A-115-08



Specimen ID: KFM08A-115-09



Specimen ID: KFM08A-115-10

